



An investigation of the structural and magnetic properties of electrodeposited $\text{Co}_x\text{Re}_{100-x}$ films

G.A. Jones^{a,*}, C.A. Faunce^a, D. Ravinder^{b,1}, H.J. Blythe^b, V.M. Fedosyuk^c

^a*Joule Laboratory, Department of Physics, The University of Salford, Salford M5 4WT, UK*

^b*Department of Physics, The University of Sheffield, Sheffield S3 7RH, UK*

^c*Institute of Solid State Physics and Semiconductors of the Belorussian Academy of Science, P. Brovki 17, 220072 Minsk, Belarus*

Received 9 July 1997

Abstract

$\text{Co}_x\text{Re}_{100-x}$ thin-film alloys with x in the range 4–100 have been prepared by the technique of electrodeposition. Deposition conditions were selected in such a manner as to attempt to produce inhomogeneous alloys from two totally miscible elements. X-ray and TEM investigations have revealed that the alloys, which were partially crystalline with an HCP structure, also contained an amorphous phase. SQUID magnetometry has been performed on the samples in the temperature range 2–300 K and in fields of up to 5 T. A magnetic behaviour has been observed which, at low Co concentrations, is compatible with superparamagnetism in the crystalline phase, whereas for higher Co concentrations, the alloys are ferromagnetic. © 1998 Elsevier Science B.V. All rights reserved.

Keywords: Electrodeposition; Inhomogeneous alloys; Thin films – alloys; Transmission electron microscopy

1. Introduction

Considerable interest has recently been aroused in the fabrication and properties of nano-sized particles of magnetic materials. This has resulted in both novel techniques and exotic structures, e.g. Petit and Pileni [1] have reported the in situ

synthesis of particles of Co_2B in reverse micelles of sodium bis (2-ethyl hexyl) sulphosuccinide and Hong et al. [2] have demonstrated the formation of nano-sized particles of HCP cobalt in a polymer matrix. These types of samples form part of a wider spectrum of so-called inhomogeneous or granular structures. Such systems are known to show ‘giant magnetoresistance’ (GMR), an effect which is of considerable relevance to the magnetic recording industry [3].

Generally, the granular samples which exhibit GMR consist of alloy films of two immiscible metals, e.g. CuCo [4], in which nano-sized single-domain

* Corresponding author. Fax: +44 161 745 5903; e-mail: g.a.jones@physics.salford.ac.uk.

¹Permanent address: Department of Physics, University of Osmania, Hyderabad, India.

particles are dispersed in a non-magnetic matrix. Whereas the bulk of the investigations on these materials have focused on films or multilayers made by sputtering, or other high-vacuum techniques, there has, nevertheless, been a steady flow of papers on samples prepared by electrodeposition (ED). Although ED remains a minority preparation technique, perhaps because it is not considered possible to prepare samples of a purity comparable with that obtained in high-vacuum methods, it has, nevertheless, been used to fabricate a variety of magnetic materials; these range from soft amorphous films of CoWFe [5] to permalloy, which is used in the fabrication of recording heads [6], and also to multilayers [7]. One of the principal merits of ED, apart from simplicity and economy of resource, is that by varying the exact conditions of deposition, it is possible to ‘fine-tune’ the properties of the layer to suit specific requirements.

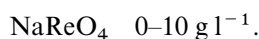
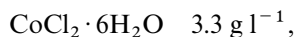
Very little work seems to have been reported on alloys of CoRe; in the literature we have been unable to find any reports of investigations into the magnetic properties of the bulk alloys, although a number of investigations of CoRe multilayers [8–10] and super-lattices [11–13] have been carried out, when the growth technique has been either high-vacuum deposition or sputtering. Depending upon the thickness of the intervening Re spacer layer, the Co layers may show either ferromagnetic or antiferromagnetic coupling.

In the present paper, we present some initial structural results, mainly obtained with transmission electron microscopy (TEM) and some concomitant magnetic data on CoRe films grown by ED; this, to the best of our knowledge, is the first work to be reported on non-layered CoRe alloys. The alloy constituents, Co and Re, were deliberately chosen because both metals possess the same structure, HCP, and are known to be totally miscible in equilibrium in the bulk [14]. This means that, under normal deposition conditions, one would not expect to produce a granular alloy. Our aim was, therefore, to establish whether, by choosing appropriate conditions for ED, it was possible to produce inhomogeneous alloys from miscible components since, if this were successful, it would open up a new class of materials in which, in principle, GMR could be observed.

2. Experimental details

2.1. Sample preparation

Films of $\text{Co}_x\text{Re}_{100-x}$ for both magnetic and TEM studies were deposited, in Minsk, on high-quality commercial copper foil and those for X-ray investigations onto ceramic substrates, the latter having previously been coated with a non-magnetic layer of NiP. From experience gained by the electrodeposition of CoW alloys [5], which are only partially miscible, we have found that, in order to prepare inhomogeneous alloys from miscible elements, we have to deposit at conditions close to equilibrium; in this case, this means conditions of high pH and low current-density. The electrolytic bath had a pH of 6.95 and deposition was performed, using a two-electrode configuration, at 50°C with a current density of 7.5 mA cm^{-2} . In the present work, the electrolytic plating bath contained the following solution:



Immediately prior to deposition, the Cu substrates were washed in detergent and then slightly etched in a 5% solution of HCl. After deposition, the samples were promptly dried in a stream of air in order to prevent surface contamination. The bath conditions were set to give a nominal film thickness of 130 nm, but no independent check of actual thickness was available. However, judging by the visual appearance of the films, they were not of uniform thickness, thus confirming that this alloy system is not an easy one to deposit, particularly so for high Re content. In the high Re regime therefore, it is unlikely that a film thickness of 130 nm was attained and, indeed, despite optimizing conditions, it proved impossible to deposit pure Re onto the substrate. Possible causes for such a failure, and

other details of the ED mechanism, are discussed in Ref. [15]

The composition of the alloy was controlled by the concentration of NaReO_4 in the electrolyte and for values (in g l^{-1}) of 0, 0.1, 0.3, 0.5, and 1.0 the corresponding atomic percentages of Re in the alloy were found, by chemical analysis, to be 0, 7, 30, 50, and 96, respectively.

2.2. Structural and magnetic measurements

Details of film composition were compiled using both X-ray and chemical analysis. For the X-ray analysis of as-deposited samples, we used Co K α radiation with a graphite monochromator and a Dron-3M instrument. The TEM investigations were carried out in Salford on a 300 kV JEOL 3010 microscope fitted with an X-ray microanalysis facility. Specimens for microscopy were prepared by initially cutting out 3 mm discs by spark erosion; these were then dimpled and ion-beam thinned. Obviously the ion beam was incident on the substrate surface and the procedure terminated once a hole had appeared in the sample. As is well known, this method of thinning can produce post-deposition artefacts and this fact must be borne in mind when the micrographs are interpreted. At this stage of the work, we have confined our TEM investigations to a study of two compositions only, viz. $x = 4$ and 50, whereas the magnetic measurements extended over a wider composition range.

Magnetic measurements were made in the temperature range 5–300 K, and in certain circumstances extended down to 2 K, and in fields of up to 5 T using a quantum design SQUID magnetometer. Measurements of magnetic moment as a function of field for various temperatures were made, together with the technique of zero-field-cooled (ZFC) and field-cooled (FC) low-field susceptibility measurement. In order to correct for the effect of the substrates which, especially at high fields and low temperatures, made significant contributions to the SQUID signal, measurements were also made on identical Cu sheets on which no films had been deposited. A comparison was also made of the commercial sheeting used for the present substrates with spectrographically pure Johnson Matthey Cu in rod form.

3. Experimental results

3.1. Structural data

For alloy films with x in the range $50 < x < 100$, traces from the diffractometer reveal several sharp X-ray peaks which can be indexed to a single HCP phase, the $\{10\bar{1}0\}$ reflection being the most intense. As x decreases within this range, the peaks shift to lower Bragg angles. This observation is consistent with the HCP lattice expanding to accommodate the larger Re atoms.

For $x \leq 50$, a further significant change is noted insofar as the peaks begin to broaden. At the highest Re concentration ($x = 2$) all traces of individual peaks are lost and only a single very broad peak is observed. This we take to indicate that the deposited film is now in a mostly amorphous state. Micrographs of $\text{Co}_{50}\text{Re}_{50}$ demonstrate a microstructure which appears to vary from one area to another on the same thinned sample: this probably reflects local variations in plating and/or non-uniformity of coating thickness. To illustrate this point, some micrographs are presented in Fig. 1a–Fig. 1c, together with a typical diffraction pattern, Fig. 1d. The most noticeable feature of Fig. 1a is the series of channels, in light contrast, which sub-divide the entire area. The channel width is remarkably uniform at about 1 nm. Contrary to a simple interpretation, the channels do not delineate individual grains because in some cases, e.g. at A, continuity of lattice plane direction is conserved on traversing a channel. We do not consider the channel system to be an artefact of the ion-milling, but rather a manifestation of initial irregular growth in an area of sample where the coating is thin. Fig. 1b and Fig. 1c, on the other hand, are taken from areas with a thicker coating of film. Here, the channel system is less conspicuous and the gradations in contrast present a distinct ‘mottled’ aspect: patches, in darker contrast, are interspersed with a ‘lighter matrix’. The mottled appearance is seen best in Fig. 1b where the patches have a reasonably uniform size in the range 5–12 nm. In Fig. 1c, however, taken at the same magnification, the patches are much larger, more irregular and often contain a sub-structure. The

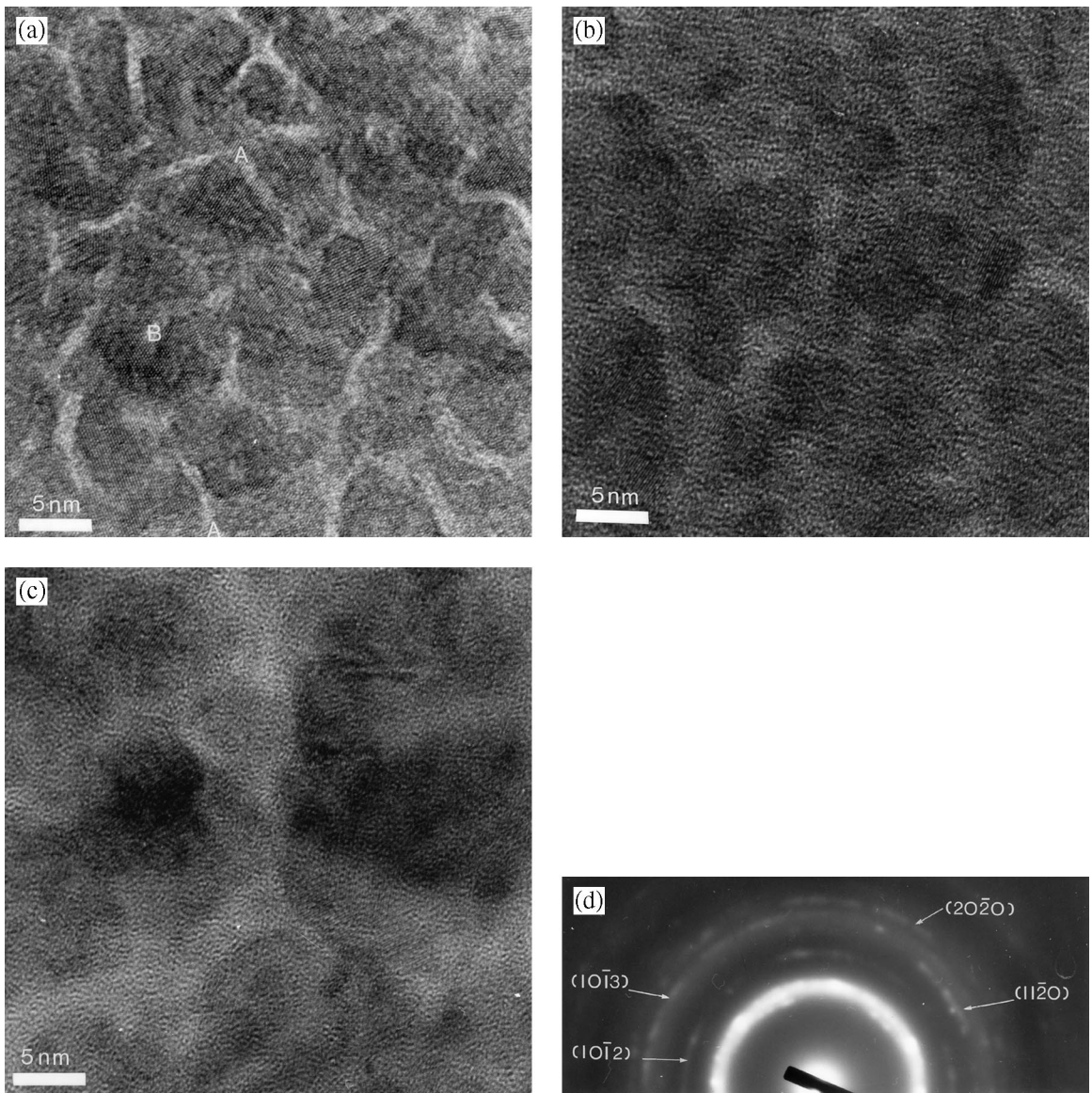


Fig. 1. (a)–(c) Micrographs of electrodeposited $\text{Co}_{50}\text{Re}_{50}$ and (d) electron diffraction pattern with indexing of HCP reflections.

matrix has a worm-like structure typical of an amorphous material [18].

Lattice fringes are readily visible over much of the area shown in Fig. 1a and these were used to help identification of the crystal structure of the film. In principle, this should present no problem because the nominal constituents of the layers are

Co and Re. However, the detector in the microscope picked up X-ray peaks from Cu as well as those from Co and Re. The possibility that the fringes observed originate from Cu has been considered, but rejected, for the following reason. In the region marked B, three sets of superposed fringes are clearly visible, of equal spacing

0.225 ± 0.007 nm, lying at angles of 60° to each other. This value of inter-planar spacing is somewhat greater than that of the maximum of 0.2087 nm for the {111} planes found in Cu. Moreover, no zone axis is possible in a cubic lattice whereby three sets of symmetrically disposed {111} planes can be imaged simultaneously from a single grain. It should be noted, however, that the {220} planes of Cu can be so arranged, but the inter-planar spacing is much too small. However, such a disposition is possible in an HCP lattice provided that the basal plane is normal to the incident electron beam: fringes from three sets of equally inclined {10 $\bar{1}$ 0} planes may be imaged in this case. The inter-planar spacings for the {10 $\bar{1}$ 0} planes in pure Co and Re, see Table 1, are 0.2169 and 0.2388 nm, respectively, and that for Co₅₀Re₅₀, assuming Vegard's law, is 0.2280 nm, which is close to the observed value. Measurements on the other regions of Fig. 1a give fringe spacings that lie between 0.213 and 0.239 nm. The latter value is outside that for Co₅₀Re₅₀ but close to that of the {10 $\bar{1}$ 0} planes of pure Re. An error of at least 3% must be attached to these measurements of *d*-spacings, but it is also possible that the deposited films have local fluctuations in composition. *d*-spacings from Fig. 1b and Fig. 1c were found to be in the range 0.211–0.214 nm, close to that for the {0002} planes of Co₅₀Re₅₀.

The diffraction pattern (Fig. 1d) reveals a strong inner halo, containing some spots, together with some fainter, fairly diffuse, outer reflections. In fact, the rings can be readily indexed, as indicated, to an HCP structure with *d*-spacings that lie between

those of pure Re and Co₅₀Re₅₀. A precise measurement is made difficult by the diffuseness of the rings. One possible origin of the diffuseness is compositional variations which obviously give rise to local variations in lattice parameters. An alternative explanation is the presence of a low-dimensional structure. Certainly, the presence of such a structure is suggested by the micrographs in Fig. 1b and Fig. 1c and X-ray data from as-deposited films which revealed broad peaks. Moreover, the inner halo of Fig. 1d is indicative of an amorphous phase. The spots at the inner and outer edges of the halo correspond closely to the {10 $\bar{1}$ 0} and {10 $\bar{1}$ 1} reflections of the HCP crystalline phase.

It will be remarked that the outer (HCP) reflections are not of uniform intensity, but contain some 'texture'. A 20 μm aperture was used in all the diffraction studies, which means that the sample specimen area has a spatial extent of the order of 1 μm (allowing for the magnification of the objective lens) i.e. much larger than the grain size. Non-uniform intensity in diffraction rings can be indicative of a microstructural texture in the film. One possible origin of such a texture lies with the Cu substrate which has a comparatively large grain size (>>1 μm). If the deposited film attempts to replicate the underlying substrate grain structure, this could lead to local clusters of HCP crystallites which share a common crystallographic orientation. As a consequence, the sampled region will not be completely random. Of course, such an explanation also accounts for the spots in the vicinity of the halo. This type of phenomenon was clearly evident in our previous work on CuCo alloys [20].

A high-resolution micrograph of the Co₄Re₉₆ alloy, Fig. 2, shows no channelling but the mottling effect is now more apparent. Compared with the previous composition, the patches, in darker contrast, are smaller, of the order of 3 nm in size. Lattice fringes are best seen in these dark contrast regions, but are not confined to them. On the whole, the fringes are less distinct than in Co₅₀Re₅₀ which makes measurement difficult. An exception is found in the area marked A where the fringe spacing is 0.214 nm which is reasonably close (1.5%) to the {10 $\bar{1}$ 1} reflection of Re.

The electron diffraction pattern, inset to Fig. 2, reveals some interesting features: similar to the case

Table 1
d-spacings for Co, Re and Co₅₀Re₅₀; those for Co₅₀Re₅₀ were computed assuming Vegard's law

{ <i>hkl</i> }	Co <i>d</i> (nm)	Re <i>d</i> (nm)	Co ₅₀ Re ₅₀ <i>d</i> (nm)
10 $\bar{1}$ 0	0.2169	0.2388	0.2280
0002	0.2045	0.2226	0.2137
10 $\bar{1}$ 1	0.1916	0.2105	0.2012
10 $\bar{1}$ 2	0.1488	0.1629	0.1599
11 $\bar{2}$ 0	0.1253	0.1380	0.1316
10 $\bar{1}$ 3	0.1154	0.1262	0.1208
20 $\bar{2}$ 0	0.1085	0.1194	0.1140

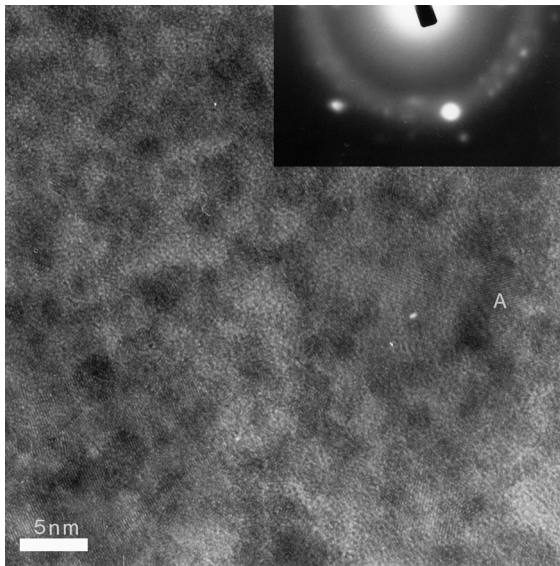


Fig. 2. Micrograph and electron diffraction pattern (inset) of $\text{Co}_4\text{Re}_{96}$.

of $\text{Co}_{50}\text{Re}_{50}$, an inner halo is observed together with some faint spots at its inner and outer periphery. These spots again lie close to those expected for the $\{10\bar{1}0\}$ and $\{10\bar{1}1\}$ reflections of an HCP phase. No additional HCP rings, of the type seen in

Fig. 1d, are observed. The absence of such rings could indicate that in this film the CoRe phase is ‘less crystalline’, a result confirmed by X-ray spectra from the as-deposited films. However, one prominent diffraction spot is observed in Fig. 2 which has a $d(hkl)$ value close to that expected for the $\{10\bar{1}1\}$ reflection in the CoRe alloy.

We would expect the tendency to be for the $\text{Co}_4\text{Re}_{96}$ films, which have the highest concentration of one of the elements, in this case Re, to show a higher crystallinity than the $\text{Co}_{50}\text{Re}_{50}$ film. However, this is the reverse of what has been observed in our TEM work although, to some extent, it is compatible with our failure to deposit pure Re.

3.2. Magnetic measurements

Hysteresis loops were measured over the temperature range 5–300 K, although for reasons of time, complete loops were not always measured at every temperature. At sufficiently low temperatures, all samples investigated exhibited hysteresis. Fig. 3 gives a summary of the temperature dependence of the remanence as determined from standard hysteresis loops measured out to 5 T. The results for each sample are normalized to the value of its remanence at 5 K. Clearly, the most dilute sample investigated,

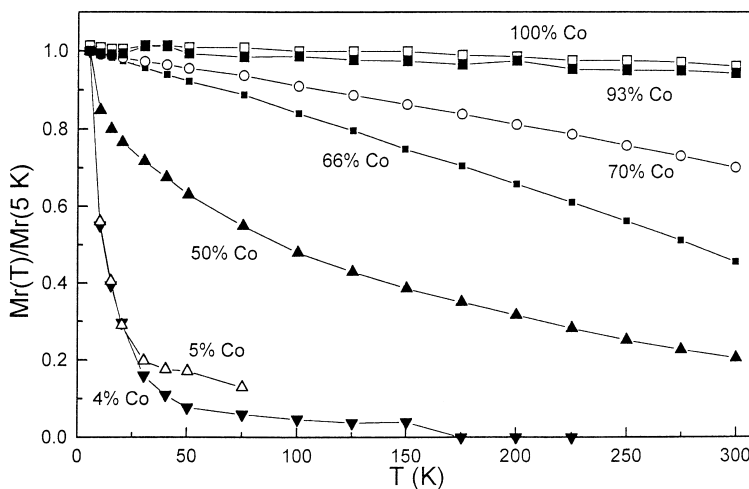


Fig. 3. Temperature dependence of the remanence for a series of $\text{Co}_x\text{Re}_{100-x}$ samples as a function of composition; values are normalized to the value measured at 5 K.

4% Co, shows the most rapid decay of remanence with increasing temperature, with hysteresis vanishing at about 175 K. With increasing Co concentration, the hysteretic behaviour extends to higher temperatures until, for concentrations of ca. 50% Co and greater, there is remanence at 300 K. Fig. 4 shows high and low-field hysteresis loops for a 50% Co sample at 300 K.

Fig. 5 shows the ZFC/FC results obtained for measurements performed on the 4% Co sample in a field of 5 mT. In these measurements, the sample was cooled in zero-field to 2 K and then measured

for rising temperatures up to 300 K. It was then immediately re-measured during cooling back down to 2 K in the same field. Since there was a strong increase of signal at low temperatures, it was decided to extend measurements down to 2 K. As the sample signals were relatively weak, and experience has shown us that, in these circumstances, there can be a significant contribution from the substrate, even though of high quality, we have repeated the same series of measurements on a blank piece of the substrate and also on a piece of Johnson Matthey spectrographically pure Cu. At

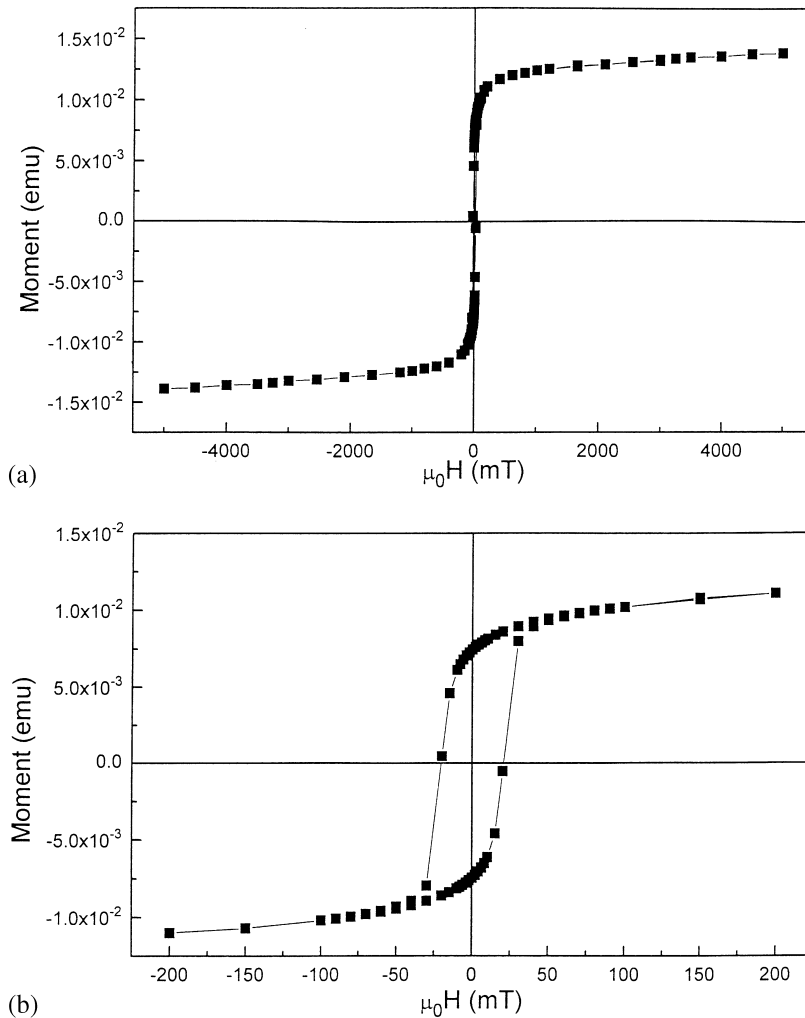


Fig. 4. Hysteresis loops for a $\text{Co}_{50}\text{Re}_{50}$ sample measured at 300 K: (a) high field and (b) low field.

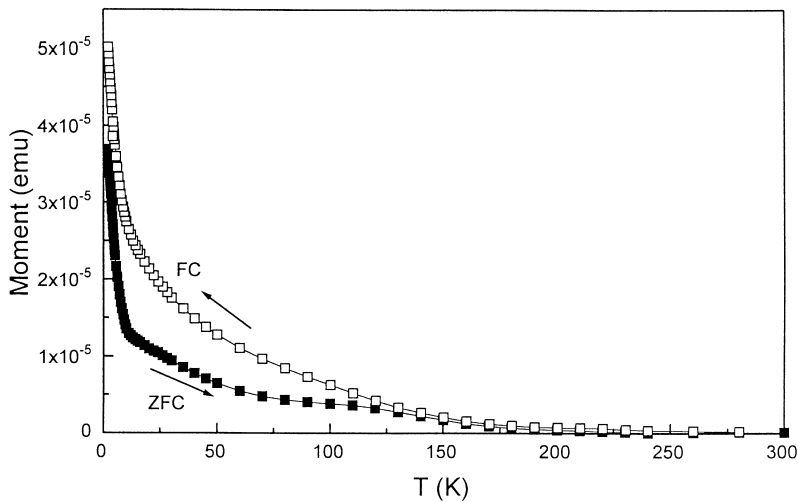


Fig. 5. Magnetization of a $\text{Co}_4\text{Re}_{96}$ film as measured in a field of 5 mT. The lower curve (■) is for the film cooled to 2 K in zero field (zero-field-cooled, ZFC), while the upper curve (□) is for the sample cooled in the measuring field of 5 mT (field-cooled, FC)

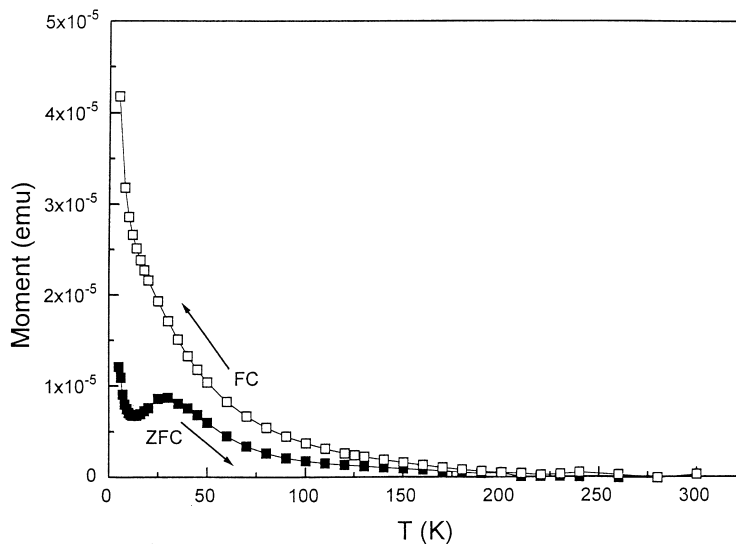


Fig. 6. Magnetization of a $\text{Co}_{30}\text{Re}_{70}$ film as measured in a field of 5 mT. The lower curve (■) is for the film cooled to 5 K in zero field (zero-field-cooled, ZFC), while the upper curve (□) is for the sample cooled in the measuring field of 5 mT (field-cooled, FC)

these low fields, the Cu appeared to behave paramagnetically with a strong increase of signal below 50 K. This behaviour was shown by both the substrate Cu and the spectrographically pure Cu; the similarity of the behaviour of both samples is evidence of the good quality of the

substrates. Nevertheless, since there is a non-negligible contribution to the SQUID signal at low temperatures and low fields, the data presented in this paper has been corrected for the influence of the substrate. In Fig. 6, we give the corresponding ZFC/FC measurements on a $\text{Co}_{30}\text{Re}_{70}$

sample and again observe the strong increase at low temperatures.

Fig. 7 gives the field dependence of the magnetization for the $\text{Co}_4\text{Re}_{96}$ at various temperatures well above that at which the hysteresis has vanished. Once again, the results have been corrected for the substrate contribution. Finally, Fig. 8 shows the data of Fig. 7 re-plotted as a function of reduced field (H/T).

4. Discussion

4.1. General comments

In a simplified approach, the effects of alloying a transition metal (TM) with a non-magnetic metal may be divided into two broad groups, depending upon whether the two elements are totally miscible or totally immiscible; these cases represent the two

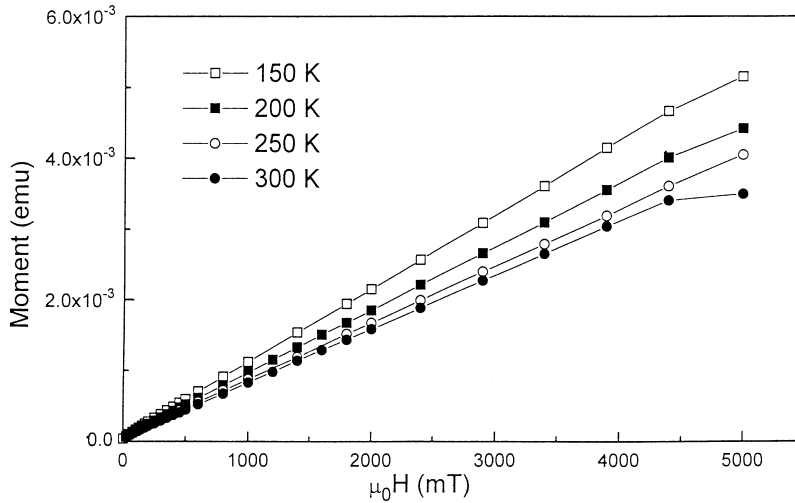


Fig. 7. Magnetization of a $\text{Co}_4\text{Re}_{96}$ film plotted at various temperatures as a function of field.

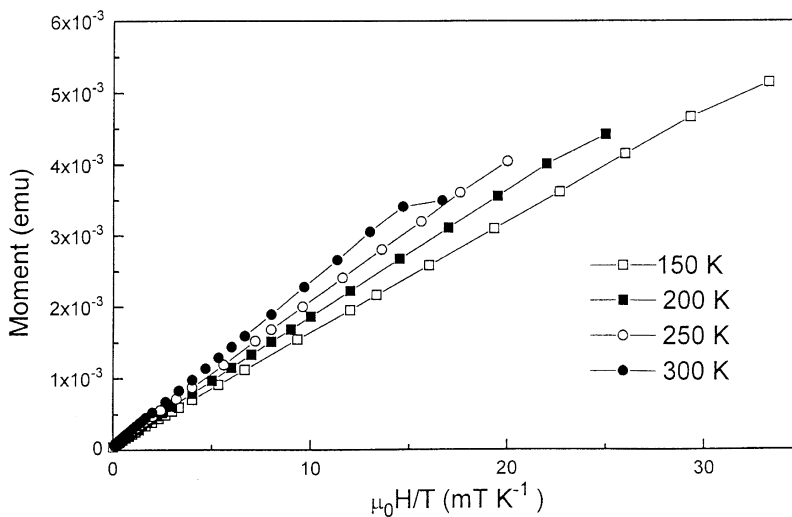


Fig. 8. Magnetization data of Fig. 7 plotted as a function of reduced field.

extremes. Usually, of course, one has a situation which is intermediate between these two extremes as the elements generally show some degree of miscibility.

4.1.1. *Totally immiscible*

In this case, if we consider an alloy which has a low concentration of the TM, and if this is ferromagnetic, we have small inclusions of the ferromagnetic element and, in sufficient dilution, expect to observe simple superparamagnetism; this situation is perhaps exemplified by the CuCo system. For sufficient dilution, which ensures the absence of interactions, below the blocking temperature, T_B , the particles are frozen in orientation, but can be aligned by a sufficiently strong magnetic field. Below T_B , therefore, hysteresis is exhibited. Above the blocking temperature, the system exhibits superparamagnetism. In the absence of interactions, the magnetization scales as a function of reduced field, i.e. plots of magnetisation versus H/T at different temperatures fall on a common curve. With increasing concentration of the ferromagnetic component, we expect to observe interaction effects, which include non-scaling of the magnetization.

4.1.2. *Totally miscible*

This extreme is, perhaps, the most interesting and also the most commonly encountered situation. In the case of a very dilute, random solid solution alloy with only a few ppm of the TM element, one observes paramagnetism, as the individual solute atoms are so widely spaced that no interactions exist between them; this is the Kondo regime. As the solute concentration is increased, the average inter-atomic separation becomes sufficiently reduced such that the long-range, oscillatory RKKY interactions due to polarization of the conduction electrons by the magnetic moments of the TM, becomes sufficiently large for inter-atomic interactions to occur. This means that a given solute atom may experience both ferromagnetic and antiferromagnetic interactions thus giving rise to frustration; this intermediate concentration region is that in which typical spin glass behaviour is observed. As the concentration of the ferromagnetic element is further increased, the average sep-

aration of the magnetic atoms decreases until the direct, short-range exchange interaction dominates the RKKY long-range interaction, the percolation threshold is reached, long-range order sets in and ferromagnetism is observed.

The characteristic behaviour of a typical spin glass is, to some extent, similar to that of a superparamagnet in that both systems exhibit hysteresis at temperatures below their so-called ‘freezing’ or blocking temperatures respectively, together with a bifurcation of their ZFC and FC curves and both show a maximum in their low-field ZFC susceptibilities. Since, of course, real spin glass materials often exhibit chemical clustering, it is also possible that superparamagnetic behaviour may obscure the effects characteristic of true spin glass behaviour; therefore, distinguishing experimentally between the two situations can be a matter of some difficulty. Furthermore, spin glass behaviour is not confined to crystalline materials but has also been observed in amorphous alloys; for reviews see Refs. [16,17]

4.2. *Present work*

4.2.1. *Structural investigation*

It is clear from the electron microscope investigations that films of both alloy compositions investigated possess an inhomogeneous microstructure. In some superficial properties, e.g. the channel system observed in $\text{Co}_{50}\text{Re}_{50}$, this is probably the result of non-uniform plating conditions. In addition, however, there is evidence that the films are only partially crystalline, a result consistent with the X-ray data taken from as-deposited samples, i.e. before thinning, which show the propensity of the alloys to become more amorphous as the Re concentration increases. Thus, in the case of $\text{Co}_{50}\text{Re}_{50}$ we are able to identify, unambiguously, electron diffraction rings which belong to an HCP phase; these rings are absent for the Co_4Re_6 specimen. On the other hand, an inner diffuse halo is present in the diffraction patterns for both compositions and this suggests the existence of an amorphous phase of CoRe as is shown by the following argument.

The angle, θ_m , at which the first elastic peak of an amorphous phase appears can be deduced from

Ehrenfest's formula [19] viz.,

$$\sin \theta_m = 1.23\lambda/2d,$$

where d is the interatomic distance and λ is the wavelength of the radiation. (This angle may not necessarily coincide with the low-angle Bragg peak of the corresponding crystalline phase.) Assuming a random, dense packing system, which is a reasonable assumption for Co and Re, then d may be taken as the atomic diameter (0.125 and 0.137 nm for Co and Re, respectively). In the case of complete segregation of the two elements, the first amorphous maxima would occur at 0.51° (Re) and 0.55° (Co) for 300 kV electrons. We cannot demonstrate from our electron diffraction patterns that segregation into two distinct amorphous phases occurs in these films, although it is well attested [18,19] in some alloys. Two broad maxima at close angles would be difficult to resolve in the microscope and, in any event, only a single amorphous phase may be present. A significant comparison is with the corresponding scattering angles for the $\{10\bar{1}0\}$ and $\{10\bar{1}1\}$ reflections, both of which have been identified in the diffraction patterns. In the case of $\text{Co}_{50}\text{Re}_{50}$ these are found, using Bragg's law, to be 0.50° and 0.56° , respectively, for 300 kV electrons, i.e. they straddle the values obtained above from the Ehrenfest relation. Thus, we may conclude that the inner halo in the diffraction patterns occurs at an angle in the vicinity of that expected from an amorphous phase of CoRe or segregated amorphous phases of either Co or Re. Electron micrographs of both alloys support this assertion. While conceding that the imaging conditions must be ideal for the formation of lattice plane images, best attained in a thin sample, we believe that the dearth of fringes in Fig. 1b, Fig. 1c and Fig. 2 is not just a reflection of instrumental deficiency, but indicates that the films comprise some regions which are crystalline and others which are not.

One final aspect of the micrographs should be noted, namely the mottling effect. This could represent gradations in thickness arising from the ion-thinning procedure but it is not apparent why the artefacts of such a process should differ between samples or even within a single sample. In fact, we have previously reported [20] a mottling phenomenon in an alloy of $\text{Cu}_{94}\text{Co}_6$ which was also pre-

pared by ED. Moreover, as in the case of $\text{Cu}_{94}\text{Co}_6$, it is observed that lattice planes are generally more distinct within patches, but they can encroach upon neighbouring lighter contrast regions. Thus, it would be an over-simplification to state that the dark patches consist of islands of crystalline matter contained within an amorphous matrix, as is the case described by Hong et al. [2] in their Co/polymer system. An alternative explanation is that the patches represent some sort of clustering process; the magnetic results confirmed this hypothesis in the case of $\text{Cu}_{94}\text{Co}_6$. With regard to the CoRe alloys, the patches or clusters in $\text{Co}_4\text{Re}_{96}$ are small, ca. 3 nm. On the other hand, the putative clusters are much bigger in $\text{Co}_{50}\text{Re}_{50}$, and of a size such that they could give rise to discernible magnetic effects. The X-ray detector on the microscope was unable to resolve any meaningful compositional difference between the clusters and adjacent areas: this was true for both compositions.

4.3. Magnetic measurements

In the electrodeposition of our samples, we have attempted, by working close to equilibrium conditions, to deposit a crystalline inhomogeneous alloy. Clearly, this was only partially successful, since our TEM measurements show that in all samples both a crystalline and an amorphous phase were present. We assume that the crystalline phase is the granular alloy with inclusions rich in Co; there is some evidence for this in the dilute Co alloys in the TEM results. If this is the case, the magnetic behaviour that we would expect is that of superparamagnetism. Part of the evidence for this is that, in the dilute 4% Co alloy, we see hysteresis at low temperatures. For the 4% Co alloy this disappears at about 170 K, Fig. 3, a temperature which we would assign to the maximum blocking temperature of the film. Also, ZFC/FC curves for that alloy, Fig. 5, show a bifurcation at that temperature. We also expect, for pure superparamagnetism, to observe a scaling of the magnetization when plotted as a function of H/T at temperatures above T_B . The fact that we do not observe such a scaling effect, Fig. 8, does not preclude superparamagnetism since such non-scaling can be attributed to interaction effects. Indeed, scaling in thin films where

superparamagnetism is claimed to occur seems to be the exception rather than the rule. On the other hand, if we consider the ZFC/FC curves for the 30% Co film, Fig. 6, the ZFC curve shows a well-defined peak at 30 K, which could be attributed to the blocking temperature corresponding to a mean particle size in a spread of particle sizes. The behaviour observed at this concentration is rather more characteristic of superparamagnetism and, in principle, would allow us to estimate particle sizes from the well-known Bean and Livingstone formula [21].

The ZFC/FC curves for both the 4% and 30% Co show strong increases in magnetization at low temperatures. One possible explanation here is that we are observing the high temperature flank of a peak with a maximum well below 2 K. It could be that this arises due to the extremely small particle sizes produced in this alloy system by the technique of ED; this would agree with the TEM measurements, but would also imply that we have a bimodal distribution of particle sizes. However, it is also possible that, in the case of the 30% Co sample, we are observing two processes: the broad peak with a maximum at 25 K together with a rapidly decaying process which has reduced to zero by about 15 K. This latter process could be due to paramagnetic behaviour of a component with a Curie temperature at very low temperature, the origin of this could possibly lie in an impurity effect in the films. On the other hand, it seems unlikely that the increase is due to interactions since the film was cooled down to 2 K in zero field and we should therefore expect an initial increase in magnetization with increasing temperature on measuring in the field of 5 mT.

With increasing Co concentration, the films become more strongly magnetic, until the 50% Co alloy exhibits classical ferromagnetism at room temperature. At this stage, we are unable to distinguish between the magnetic properties of the crystalline and amorphous phases. However, we tentatively suggest that at low Co concentrations, we could expect a spin-glass-type behaviour of the amorphous phase, which would have an overall similarity with the superparamagnetic behaviour of the crystalline component of the film.

5. Conclusions

Using the technique of electrodeposition, an attempt has been made to grow an inhomogeneous thin-film alloy from two totally miscible, HCP metals, viz., Co and Re. Films with differing Co concentrations have been investigated structurally by both X-ray diffraction and transmission electron microscopy and found to consist of a crystalline HCP phase together with an amorphous component; in the Re-rich films, the crystalline material was found to contain Co-rich clusters. A magnetic investigation of the films has led us to propose, tentatively, a superparamagnetic behaviour of the crystalline phase, with a possibility of spin glass behaviour in the amorphous component. At higher Co concentrations, the films exhibit ferromagnetism. Finally, we believe that it would be extremely interesting to investigate the magneto-resistive behaviour of these thin-film materials.

Acknowledgements

The authors are grateful to Mr. Brian Ashworth for help with sample preparation. Our thanks also go to Professor G.A. Gehring for discussions and to Professor P.J. Grundy for a critical reading of the manuscript. Two of us (VMF, DR) acknowledge financial support from the Royal Society. This work was supported by the EPSRC under grant numbers GR/H65320, GR/J25338 and GR/K53598.

References

- [1] C. Petit, M.P. Pileni, *J. Magn. Magn. Mater.* 166 (1997) 82.
- [2] J. Hong, E. Kay, S.X. Wang, *IEEE Trans. Magn.* 32 (1996) 4475.
- [3] S.S. Parkin, *Appl. Phys. Lett.* 60 (1992) 512.
- [4] J.Q. Xiao, J.S. Jiang, C.L. Chien, *Phys. Rev. Lett.* 68 (1992) 3749.
- [5] V.M. Fedosyuk, J.M. Riveiro, *J. Non-Cryst. Solids* 143 (1996) 99.
- [6] C. Tsang, H. Santini, D. McCowan, J. Lo, R. Lee, *IEEE Trans. Magn.* 32 (1996) 7.
- [7] M. Alper, K. Attenborough, R. Hart, S.J. Lane, D.S. Lashmore, C. Younes, W. Schwarzacher, *Appl. Phys. Lett.* 63 (1993) 2144.

- [8] P.P. Freitas, L.V. Melo, I. Trindade, M. From, *J. Magn. Magn. Mater.* 116 (1992) 92.
- [9] I.G. Trindade, P.P. Freitas, *J. Magn. Magn. Mater.* 121 (1993) 286.
- [10] L.V. Melo, P. Monteiro, P.P. Freitas, *J. Magn. Magn. Mater.* 121 (1993) 390.
- [11] Y. Huai, R.W. Cochrane, M. Sutton, *J. Appl. Phys.* 73 (10) (1993) 5530.
- [12] J.B. Sousa, R.P. Pinto, B. Almeida, M.E. Braga, P.P. Freitas, L.V. Melo, I.G. Trindade, *J. Appl. Phys.* 75 (10) (1994) 6551.
- [13] N. Barradas, J. Leal, H. Wolters, M.F. da Silva, A.A. Melo, J.C. Soares, L. Melo, P. Freitas, B. Swinnen, M. Rots, *J. Magn. Magn. Mater.* 121 (1993) 80.
- [14] M. Hansen, *Constitution of Binary Alloys*, McGraw-Hill, New York, 1958.
- [15] V.M. Fedosyuk, M.U. Sheleg, O.I. Kasyutich, M.M. Malyushi, *Phys. Stat. Sol. (a)* 115 (1989) 279.
- [16] D. Chowdhury, *Spin Glasses and Other Frustrated Systems*, World Scientific, Singapore, 1986.
- [17] K. Binder, A.P. Young, *Rev. Mod. Phys.* 58 (1986) 801.
- [18] M. Audier, P. Guyot, J.P. Simon, N. Valignat, *J. de Phys.* 46 (C-8) (1985) 433.
- [19] R. Yavari, S. Nishitani, P. Desre, P. Chieux, *Zeit. für Phys. Chemie* 157 (1988) 103.
- [20] H.J. Blythe, G.A. Jones, V.M. Fedosyuk, *J. Mater. Sci.* 31 (1996) 6431.
- [21] C.P. Bean, J.D. Livingstone, *J. Appl. Phys.* 30 (1959) 120.